Direct Observation of Anisotropic Interparticle Forces in Nematic Colloids with Optical Tweezers

Makoto Yada,[1,*] Jun Yamamoto,[1] and Hiroshi Yokoyama[1,2]

[1]*Yokoyama Nano-structured Liquid Crystal Project, ERATO, Japan Science and Technology Corporation, 5-9-9 Tokodai, Tsukuba, Ibaraki, 300-2635, Japan*

[2]*Nanotechnology Research Institute, National Institute of Advanced Industrial Science and Technology, 1-1-1 Umezono, Tsukuba, Ibaraki, 305-8568, Japan*

(Received 23 November 2003; published 3 May 2004)

Interparticle forces in a nematic liquid-crystal colloid have been directly observed by the dual beam laser trapping method with pN sensitivity. We introduce two different types of spatial distributions of forces, detected between the particles accompanied by hyperbolic hedgehog defects. These force distributions lead to specific particle arrangements, which are both stabilized by the balance of the orientational stress field of nematics. On the basis of these results, we propose novel artificial construction for multiparticle regular arrangements.

DOI: 10.1103/PhysRevLett.92.185501 PACS numbers: 61.30.Jf, 82.70.Dd, 87.80.Cc

Dispersions of particles in liquid crystals (LCs), referred to as liquid-crystal colloids or emulsions, have attracted considerable scientific and technological attention in recent years [1–4]. Unlike conventional colloids and emulsions, the interparticle forces in the LC media become highly anisotropic and long ranged, making it possible to spontaneously develop a variety of ordered arrangements of particles. A single particle breaks the continuous rotational symmetry of a liquid crystal, and, when the surface anchoring is sufficiently strong, it behaves topologically as a core of an orientational defect yet with a much lower energy of formation because of its nonsingularity [5–7]. Various types of topological defects, such as a hyperbolic hedgehog, a Saturn ring, and boojums, have been recently reported in dispersions of water droplets in a nematic phase [1,8,9]. The particularly unusual multiparticle behavior is to form linear chains of water droplets having hyperbolic hedgehog defects, without direct contact between the droplets [1]. The hyperbolic hedgehog defect is created to one side of a droplet with a homeotropic anchoring surface (that is, a radial hedgehog defect) along the surrounding director field, in order to satisfy a total topological charge of zero. Thus induced distortion of the liquid crystalline order assumes a dipolar property, which leads to the chain formation owing to the balance of long-range dipolar attractive and short-range defect-mediated repulsive interactions. In other systems of LC emulsions, there are some attractive reports about spontaneously formed three-dimensional defect structures, which are composed of water droplets and nematic [2] or cholesteric fluids [4,10]. Liquid-crystal dispersions can be thus expected to show further new liquid-crystal structures and unique phenomena [11], owing to the interparticle and/or particle-LC interactions.

In this Letter, we report quantitative evaluation of anisotropic interactions between solid particles dispersed in a nematic fluid, particularly in various positional configurations of two particles in a two-dimensional plane. The interparticle forces of a pN order in each specified configuration were examined by using a laser trapping method [12,13]: a micron-scale particle can be trapped on a focused laser beam owing to the radiation pressure generated by the difference of the refractive indices between the particle and the medium. We show two different types of anisotropic spatial distributions of trapping forces, interacting between two particles with hyperbolic hedgehog defects. One force distribution, which leads to a linear chain formation of the particles [1], was compared with a theoretical prediction for the dipolar attractive interaction [6]. On the other hand, the other distribution causes one stable particle arrangement, which is not a linear chain. On the basis of these two types of force distributions, we will finally propose and show examples of artificial construction of multiparticle regular arrangements in nematic colloids.

As our solid particle/LC system, we prepared cross-linked polystyrene (PS) particles (radius a: $7.5 \sim 15$ μm, from Duke Science) and a nematic LC (ZLI-4792, N 96.5 °C I, from Merck). The refractive indices of PS and ZLI-4792 at the measurement temperature, 70 °C, are 1.59 and 1.49, respectively, where the value of the nematic is the weighted average of the ordinary and extraordinary refractive indices (1.47 and 1.52, respectively), evaluated with an Abbe refractometer (wavelength: 589 nm). The surface of PS particles was treated with the surfactant (FS150, from Dainippon Ink & Chemicals) to promote homeotropic orientation of LC molecules by immersing in its aqueous solution and then dried. The particles and ZLI-4792 were simply mixed and sandwiched with glass substrates having planar anchoring surfaces (from EHC Co., Ltd., Japan). The sample thickness was fixed at 50 μm by using spacer beads.

For the dual optical traps, we applied a pair of linearly polarized laser beams (wavelength: 1064 nm) with polarizing directions perpendicular to each other, which were

adjusted with a beam splitter and a half-wave plate, in order to simultaneously manipulate two particles. The position of each laser spot, focused through an objective lens (50 ×, NA = 0.42), was computer controlled by two galvano mirrors. The irradiation intensity of each laser beam was changed within 1 ~ 90 mW by the control of the main laser power and ND filters. The motion of particles was monitored with a charge coupled device camera by tacking the trajectory of a particle when released from a given configuration. Using the dual beam laser trap, we first arranged two interacting particles in their initial positions, and then gradually reduced the laser power of one of the two beams until the particle started to be released. The minimum laser power $I_{\min}$ that is necessary to hold the particle, and the angular direction ϕ along which the particle started moving, were systematically examined to make a force map around the fixed particle. The relation between $I_{\min}$ and the trapping force F was separately calibrated in an isotropic fluid on the basis of the Stokes law, $F = 6\pi\eta a v$, where η, a, and v are the viscosity of the liquid, the particle radius, and the particle velocity in the medium, respectively. This method enables us to measure the interparticle force without the contribution of hydrodynamic interactions owing to the motion of particles.

Shown in Fig. 1 is the characteristic motion of a PS particle ($a \sim 11.6$ μm) for the linear chain formation after the release from the laser trap. As illustrated in Fig. 1(a′) [6], the hyperbolic hedgehog defect is induced by the mismatch of liquid crystalline order, that is, LC molecules are perpendicularly oriented on the surface of particles while they are uniformly aligned along z axis far from the particles. Poulin *et al.* [14] reported that two particles, forming a linear chain in equilibrium, approach head on to each other when the particles are pulled apart along z axis by a magnetic field, owing to the dipolar attractive interaction. Here, a laser trapping method allows us to set or approach two particles in any configurations in a two-dimensional plane. We show an example in Fig. 1(a), that two particles having the defects both on the left side are set along the direction perpendicular to the z axis. When one laser-trapped particle is moved closer to another along this direction, a repulsive force can be examined between these particles. After releasing from the configuration shown in Fig. 1(a), the particles start to gradually move almost along the z axis in the opposite direction, and then they approach while moving in an arc [Fig. 1(b)], which leads to a chain formation of the particles along the z axis [Fig. 1(c)]. These results clearly indicate the presence of anisotropic spatial distribution of interparticle forces on micrometer scale, owing to the director field distorted around each particle. Figure 1(c′) illustrates the scheme of the director field of a linear chain [6], which has a smaller distortion than that of Fig. 1(a′), by the particles lying a single line and possibly approaching.

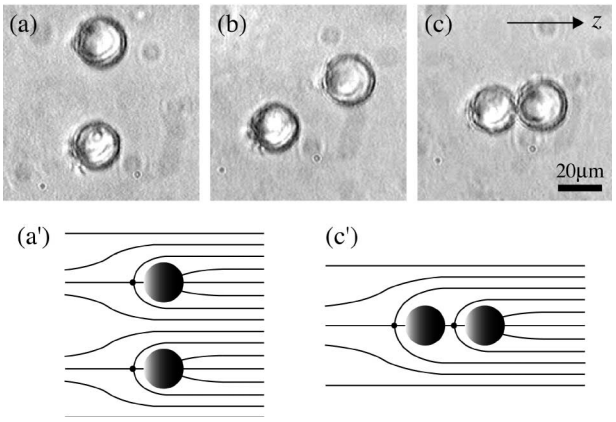

FIG. 1. Motions of PS particles to a linear chain formation. (a)–(c): Optical microscope images, monitored after the release from the laser trap. z axis: the alignment direction of nematics far from the particles. (a′) and (c′) are predicted schemes of the director fields in (a) and (c), respectively.

Next, we investigated a two-dimensional distribution of the interparticle forces, in the case that a linear chain was finally formed. Figure 2(a) shows the force map between two particles ($a \sim 11.6$ μm) as a function of the center-to-center distance R ($R/a \sim 2.5$, 3.3, 4.2, and 4.9) and the azimuthal angle θ [$0 \le \theta \le 180°$, as shown in Fig. 2(a)]. The length and the direction of an arrow in Fig. 2(a) indicate the strength F and the direction ϕ of the trapping forces, respectively. The clear interparticle attractive forces appear along z axis ($\theta = 0°$ and 180°), while the weak repulsion exists along the direction perpendicular to z axis ($\theta = 90°$). In the intermediate angle range, the released particle tends to move toward $\theta = 0°$ or 180°, along the circumference of the trapped one. These results mean that the linear chain can be formed wherever these particles are initially set, except on the line strictly perpendicular to z axis.

Lubensky *et al.* [6] have formulated a theory of elastically mediated forces between the particles with hyperbolic hedgehog defects; the theoretical predictions have not yet been experimentally examined, however. Here, we compare our force map obtained above [Fig. 2(a)] with the theoretical distribution of the dipolar attractive forces between the particles. We ignore the quadrupolar interparticle interaction, whose contribution to the force is much smaller than that of the dipolar interaction [6].

When two particles of radius a, positioned at $r(0, 0)$ and $r(r, \theta)$, are interacting via the dipole-dipole forces, the interaction energy is expressed in terms of the dipole moment p_z and the dipole-dipole potential $V_{pp}(r)$ as

$$U(\mathbf{r}) = 4\pi K p_z^2 V_{pp}(\mathbf{r}). \quad (1)$$

Here, K is the Frank elastic constant for the nematic director field in the one-constant approximation [15], with $p_z = 2.04a^2$ and $V_{pp}(\mathbf{r}) = r^{-3}(1 - \cos^2\theta)$. The interparticle force can be calculated by $\mathbf{F} = -\partial U/\partial \mathbf{r}$, then

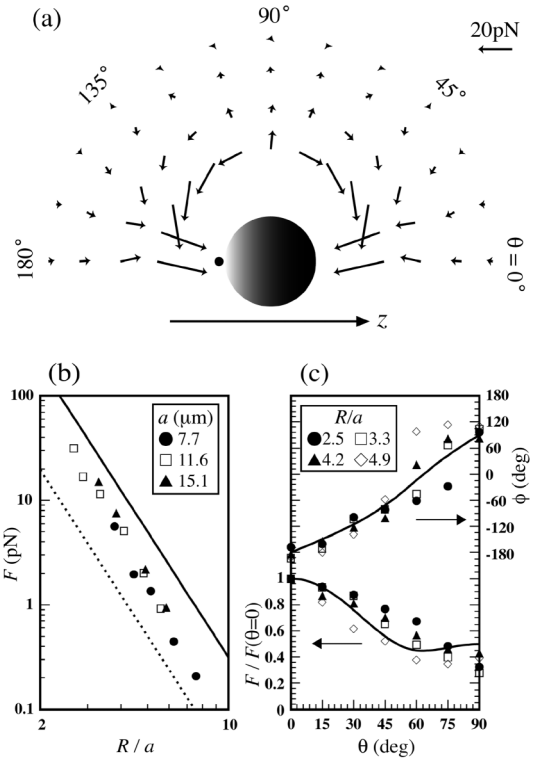

FIG. 2. Spatial distribution of the interparticle forces F, in case that a linear chain is formed (a). Force map between two particles ($a \sim 11.6$ μm), measured with changing R/a ($\sim$2.5, 3, 3. 4.2, and 4.9) and θ ($0 \sim 180°$). (b). Dependence of F on R/a along z axis ($\theta = 0°$), in various R and a. Solid and dotted lines: $F = 100\pi K(a/R)^4$ ($K = 10$ and 1 pN, respectively). (c) θ dependence of the normalized F and f ($a \sim 11.6$ μm), where ϕ is the direction pointed by arrows in (a), which was defined as the angle from the positive z axis. Each solid curve is the theoretical prediction, calculated from Eq. (2).

$$\mathbf{F} = \frac{12\pi K\, p_z^2}{r^4}\{(1 - 3\cos^2\theta)\mathbf{e}_r - 2\cos\theta\sin\theta\mathbf{e}_\theta\}, \quad (2)$$

where e_r and e_θ are orthogonal unit vectors. Equation (2) can predict the motion of the particle positioned at $r(r, \theta)$. For example, the substitution of $\theta = 0$ and $r = R$ into Eq. (2) provides the dependence of the dipolar force F on the distance R along z axis as $F \sim 100\pi K(a/R)^4$. Figure 2(b) shows the experimental results of interparticle forces along z axis for various a and R, together with two theoretical lines of $F = 100\pi K(a/R)^4$ with an assumption of $K = 1$ or 10 pN as typical values in nematics [15]. From Fig. 2(b), indeed, we find that the measured trapping forces are nearly proportional to R^{-4}, moreover the quantitative agreement is quite notable. On the other hand, Fig. 2(c) shows the θ dependence of the trapping force F as well as the release direction ϕ, which is pointed by arrows in Fig. 2(a) for various R ($a \sim 11.6$ μm). Here, ϕ is defined as the angle from the positive z axis ranging between $-180°$ and $+180°$, and the data of F were normalized by the value at $\theta = 0°$ in the same distance R. Figure 2(c) also includes the predicted curves of F and ϕ, as obtained from Eq. (2). As already shown in Fig. 2(a), the measured trapping force F tends to decrease while the release direction ϕ changes from $-180°$ to $+90°$, with the change of θ from 0° to 90°. We can also find in Fig. 2(c) that the experimental results roughly agree with the theoretical lines. These agreements with theoretical values in Figs. 2(b) and 2(c) verify that the dipolar interaction is consistently dominant between these particles in any configurations.

Next, we consider another distinct interaction of two particles with hyperbolic hedgehog defects, under the condition that each particle has their accompanying defect on the different side, as shown in Fig. 3. When these particles were forced to approach one dimensionally along the z axis, they repulsed each other in both cases of the approach from the defect side and from the nondefect side of each particle. This can be easily explained by the dipolar repulsion between the same charges of the hedgehog distribution. On the other hand, when these two particles are set not along the z axis [for example, in Fig. 3(a)] and released from the trap, the particles tend to assume only one positional configuration shown in Fig. 3(c). Figure 4 shows the force map created under the same condition as in Fig. 2(a), which has an asymmetric spatial distribution. Fairly high attractive forces (>20 pN) are generated only around $\theta = 150°$. Moreover, the released particle, which is set at an arbitrary angle except $\theta = 0°$ or 180°, tends to move toward $\theta = 150°$ along the circumference of the fixed one. These results indicate that the particle arrangement shown in Fig. 3(c) is one of the stable structures in the nematic colloid. In $\theta = 0$ or 180°, on the other hand, the interparticle dipolar repulsion was detected as already stated, but the repulsive forces could not be precisely measured under the conditions of $R/a \sim 2.5$ and 3.3 in $q = 180°$, where the hyperbolic hedgehog defects were quite close to each other. In these conditions, we observed that the rotation of the particle took place before leaving the trap

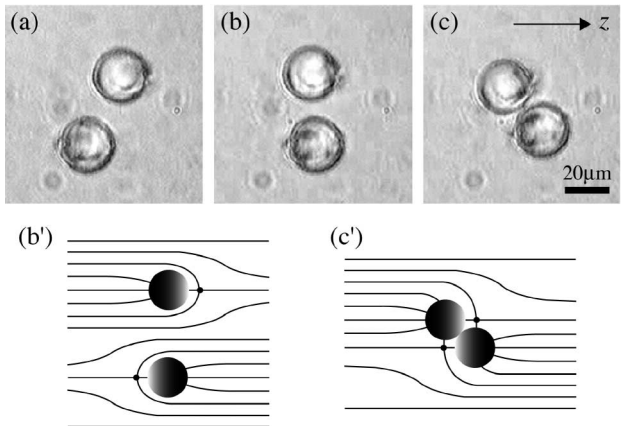

FIG. 3. Motions of the particles having the defects to the different side along the z axis. (a)–(c): Optical microscope images, monitored after the release from the laser trap. (b′) and (c′) are predicted schemes of the director fields in (b) and (c), respectively.

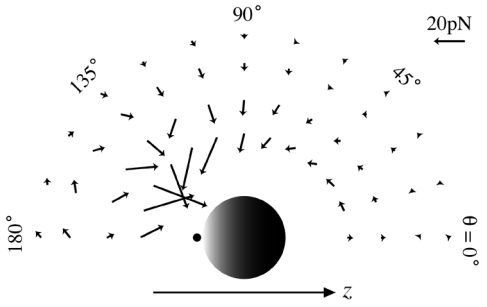

FIG. 4. Force map between two particles ($a \sim 11.9$ μm), in the case that the specific structure shown in Fig. 3(c) is formed. The experimental conditions are the same as that of Fig. 2(a).

position on reducing the laser power in such a way to avoid the closeness of these defects.

We intuitively predict the director field around the particle arrangement shown in Fig. 3(c), as illustrated in Fig. 3(c′). This arrangement will be caused by the minimization of the distortional energy of the liquid crystalline order, in the same way as a linear chain formation. Two isolated particles having the defects to the different side [Fig. 3(b′)] tend to move for the reduction of the total distortion of the director field, which leads to their unique motion [Figs. 3(a) and 3(b)] and finally their aggregation [Fig. 3(c)]. Simultaneously, the dipolar repulsive interaction is generated between the same charges of the hedgehog distribution, which prevents one particle from going onto the symmetry axis of the hedgehog distribution around another particle. As a result of these energetic requirements, the director distribution described in Figs. 3(c′) should be settled down, producing this particular arrangement of particles. We can thus conclude that the particle arrangement shown in Fig. 3(c) is another stable configuration, distinct from the linear chain.

In this Letter, we introduced two types of anisotropic spatial distributions of the trapping forces between the particles with hyperbolic hedgehog defects [Figs. 2(a) and 4], which lead to the stabilized arrangements of the particles shown in Figs. 1(c) and 3(c), respectively. The laser trapping method, furthermore, allows us to create new multiparticle configurations on the basis of their anisotropic interactions. Figure 5 shows examples of optical manipulation of multiparticles for building up the anisotropic arrangements, a zigzag chain and a Y-shape arrangement [Figs. 5(b) and 5(c), respectively], composed of four particles with hyperbolic hedgehog defects [Fig. 5(a)]. These structures were both maintained over 1 day without the laser trap, since every pair of adjacent two particles has the stable configuration shown in Figs. 1(c) or 3(c). Thus, the application of the optical manipulation to the field of liquid-crystal dispersions will enable the artificial construction of more complicated arrangements of particles. The multiparticle arrangements as shown above should probably be just a few examples of the rich variety of metastable configurations in nematic colloids. As indicated in this Letter, the intricate balance of anisotropic forces mediated by the liquid crystalline order play the decisive role.

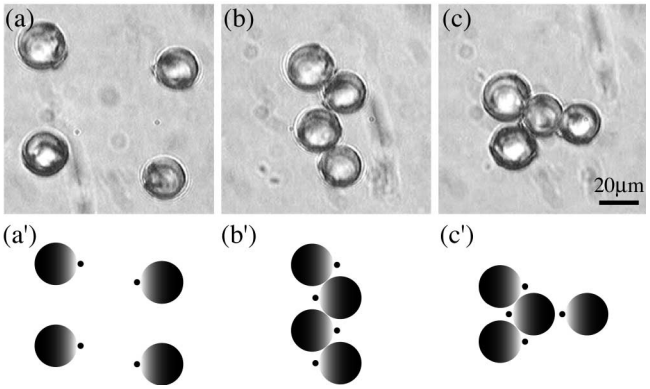

FIG. 5. Artificial construction of the anisotropic arrangements composed of four particles with hyperbolic hedgehog defects [shown in (a)]. A zigzag chain and a Y-shape arrangement were created [(b) and (c), respectively], where every pair of adjacent two particles has the stable configuration shown in Figs. 1(c) or 3(c)

We gratefully acknowledge Dr. J. Fukuda for his helpful comments and discussion.

*To whom correspondence should be addressed.

[1] P. Poulin, H. Stark, T. C. Lubensky, and D. A. Weitz, Science **275**, 1770 (1997).
[2] J. Yamamoto and H. Tanaka, Nature (London) **409**, 321 (2001).
[3] T. Bellini, M. Caggioni, N. A. Clark, E. Mantegazza, A. Maritan, and A. Pelizzola, Phys. Rev. Lett. **91**, 085704 (2003).
[4] M. Yada, J. Yamamoto, and H. Yokoyama, Langmuir **18**, 7436 (2002).
[5] P. M. Chaikin and T. C. Lubensky, *Principles of Condensed Matter Physics* (Cambridge University Press, Cambridge, 1995).
[6] T. C. Lubensky, D. Pettey, N. Currier, and H. Stark, Phys. Rev. E **57**, 610 (1998).
[7] B. I. Lev, S. B. Chernyshuk, P. M. Tomchuk, and H. Yokoyama, Phys. Rev. E **65**, 021709 (2002).
[8] P. Poulin and D. A. Weitz, Phys. Rev. E **57**, 626 (1998).
[9] O. M. Monval, J. C. Dedieu, T. G. Krzywicki, and P. Poulin, Eur. Phys. J. B **12**, 167 (1999).
[10] M. Yada, J. Yamamoto, and H. Yokoyama, Langmuir **19**, 3650 (2003).
[11] T. Yamamoto, J. Yamamoto, B. I. Lev, and H. Yokoyama, Appl. Phys. Lett. **81**, 2187 (2002).
[12] A. Ashkin, Phys. Rev. Lett. **24**, 156 (1970).
[13] Y. Iwashita and H. Tanaka, Phys. Rev. Lett. **90**, 045501 (2003).
[14] P. Poulin, V. Cabuil, and D. A. Weitz, Phys. Rev. Lett. **79**, 4862 (1997).
[15] P. G. de Gennes and J. Prost, *The Physics of Liquid Crystals* (Oxford University Press, New York, 1993), 2nd ed.